Census of Young Stars in Galactic Star Forming Region Sh2-88

Soumita CHAKRABORTY[1,*], Soumen MONDAL[1,*], Alik PANJA[1], Siddhartha BISWAS[1],
Sudip PRAMANIK[1], Dorothy MUSEO MWANZIA[1,2] and Santosh JOSHI[3]

[1] S. N. Bose National Centre for Basic Sciences, Kolkata, India
[2] University of Nairobi, Nairobi, Kenya
[3] Aryabhatta Research Institute of Observational Sciences, Nainital, India
[*] Corresponding authors: soumitach25@gmail.com; soumen.mondal@bose.res.in

Abstract

We present here the census and characterization of Young Stellar Objects (YSOs) associated with the active star-forming H II region Sh2–88 with multi-wavelength data situated in the Vulpecula OB1 association. To understand the extinction properties of the Sh2–88 region, we generate an extinction map over 20×20 arcminutes using the neighbourhood method of Gutermuth et al. (2005) from the deep near-infrared *HK* band photometric archival data of UKIDSS. We find a sizeable variable extinction over the region up to $A_V \simeq 11.7$ mag, with a median value of $A_V \simeq 4.3$ mag. The high extinction regions trace the dense filamentary structure, which was found earlier in the far-infrared and sub-mm data. Following the YSO classification scheme of Gutermuth et al. (2009), we have identified 74 YSOs in that region using *Spitzer*–IRAC data from four mid-infrared bands (3.6, 4.5, 5.8 and 8 μm) and 2MASS near-infrared *K*-band (2.16 μm) data. Among 74 YSOs, six are class I and 68 class II objects. Using IPHAS H$_\alpha$, *r*, and *i*-band photometry, we have identified 41 additional YSOs. Among these 41, four sources are common with IR excess YSOs. From the spatial distribution of YSOs, it is apparent that YSOs are primarily distributed over the relatively higher extinction regions of the cloud, and star-formation activity might be ongoing in those dense parts of the cloud.

Keywords: Star-formation, Giant Molecular Cloud, Young Stellar Object

1. Introduction

Giant Molecular Clouds are the main sites of cold and star-forming molecular gas in galaxies. These molecular clouds cover a mass range of 10^2 to $10^3 M_\odot$, with sizes ranging from 10 to 100 pc. The average temperatures and densities of these clouds in GMCs are in the range of 10–30 K and 50–100 cm^{-3} respectively. Large-scale star formation involves several physical processes spanning a vast range of physical scales: accretion phases of gas from the intergalactic medium; cooling of the gas to form a cold neutral phase; formation of molecular clouds; clumps and cores; then to stars from the subsequent contraction of the cores (Kennicutt and
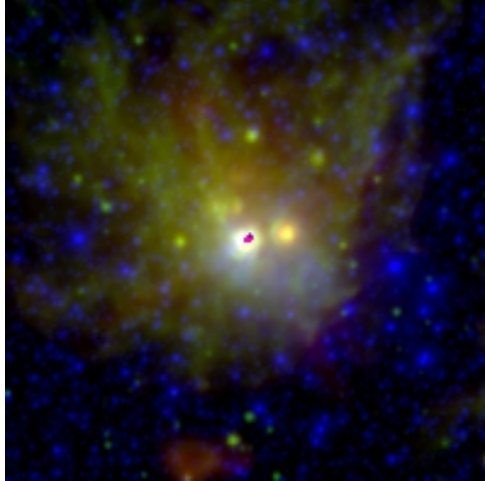
Figure 1: RGB image of Sh2–88 over 20×20 arcminutes, created using WISE $W2$, $W3$ and $W4$ bands. The molecular dust clouds are clearly traced from the mid-infrared images.

Evans, 2012). Most of the massive stars form in the OB association, where the neighbouring environment of massive stars influences via several feedback mechanisms, e.g., stellar wind, UV radiation, supernova explosion, etc. (McKee and Ostriker, 2007). The feedback mechanism may also affect star-formation by clearing away the dust and gas (Walch et al., 2013). H II regions are emission nebulae created by high ultraviolet radiation from those young and massive OB stars. The OB stars have the capability to produce the necessary UV radiation (Lyman photons) to ionize the surrounding hydrogen gas medium and create a spectacular view of H II region. A massive star plays a vital role to ionize its nearby molecular clouds and to trigger the formation of stars at the edges of H II regions. The interaction between H II regions may create a filamentary molecular cloud structure, which may induce the star-formation cores along the filament axis (Fukuda and Hanawa, 2000; André et al., 2014).

Here we studied a high-mass star-forming region of Sh2–88 in the Vulpecula OB association (hereafter Vul OB1), which was first catalogued by Morgan et al. (1953). Vul OB1 contains three H II regions, namely Sh2–86, Sh2–87, and Sh2–88 (Sharpless, 1959). Sh2–88 (hereafter S88) is a compact H II region located at the galactic coordinate $(l,b) \simeq (61.°47, 0.°10)$ at a distance of about 2.0–2.3 kpc (Billot et al., 2010; Kohno et al., 2022). S88 is excited by an O8.5V–O9.5V massive star (Deharveng et al., 2005; Cappa et al., 2002). However, the complete census of S88 is not well-studied in the IPHAS optical and *Spitzer* mid-IR data. The RGB image of S88, covering 20×20 arcminutes shown in Fig. 1 was created from Wide-field Infrared Survey Explorer (WISE) $W2$, $W3$, and $W4$ band data, where the molecular dust clouds are clearly traced from the mid-infrared images.

2. Data Sets

We have used here multi-wavelength data from archival catalogues in the infrared wavelengths based on ground as well as space telescope facilities. The near-infrared J- (1.25 μm),

H- (1.65 μm) and *K*-band (2.16 μm) photometric data were obtained from the UKIRT Infrared Deep Sky Survey (UKIDSS) Galactic Plane Survey (Lawrence et al., 2007). The *Spitzer*–IRAC mid-IR observations in the 3.6, 4.5, 5.8 and 8 μm bands (IRAC; Fazio et al. (2004)) were retrieved from the *Spitzer* archive from the legacy program *Galactic Legacy Infrared Mid-Plane Survey Extraordinaire* (GLIMPSE; Benjamin et al. (2003)). The *K*-band data of the 2MASS Point Source Catalogue (PSC;Skrutskie et al. (2006)) is also used and available with the GLIMPSE catalogue. A photometric uncertainty of ≤ 0.1 mag (SNR > 10) for all the bands was considered as a quality criterion for UKIDSS and 2MASS, while it was ≤ 0.2 mag for IRAC data. We also used data from the INT/WFC Photometric Hα Survey of the Northern Galactic Plane (IPHAS) archives for our photometric study of S88. IPHAS is an optical photometry sky survey in the Northern Milky Way in narrow-band H_α(656.8 nm), *r* (624 nm) and *i* (774.3 nm) filter bands using the wide-field camera on the 2.5-m Isaac Newton Telescope (INT) in La Palma (Drew et al., 2005). The photometric data on those bands were taken from the IPHAS DR2 catalogue (Barentsen et al., 2014). A photometric uncertainty of ≤ 0.1 mag (SNR > 10) for all the bands was considered as quality criterion for IPHAS.

3. Results and Discussion

3.1. The extinction map

An extinction map traces the dust distribution of the molecular clouds. Following the neighbourhood method of Gutermuth et al. (2005), we have created a spatial grid of size of $5'' \times 5''$ over the 20×20 arcminutes target area of S88 at the centre coordinate of RA = $19^\mathrm{h} 46^\mathrm{m} 45.7^\mathrm{s}$, DEC = $+25°12'56''$. We used the deep *H*- and *K*-band near-infrared photometry from the UKIDSS catalogue (Lawrence et al., 2007). The 20 nearest-neighbour sources are selected around the centre of the grid position, to calculate the mean and standard deviation of the $(H - K)$ colour for each grid. The 3σ outliers of the mean values of $(H - K)$ for each grid position are rejected (Panja et al., 2020, 2021, 2022). From the mean $(H - K)$ colour for each grid position, the extinction in the *K*-band is estimated from the relationship between the observed and the intrinsic colours (Flaherty et al., 2007a):

$$A_K = 1.82 \times [(H - K)_\mathrm{obs} - (H - K)_\mathrm{int}].$$

The average intrinsic colour $(H - K)_\mathrm{int}$ of the background population is taken to be ~ 0.2 mag (Flaherty et al., 2007b; Panja et al., 2021, 2022). The value of *K*-band extinction magnitude A_K is converted to the visual extinction, A_V, using $A_V = A_K/0.112$ (Rieke and Lebofsky, 1985). The visual extinction map covering 20×20 arcminutes around S88 is shown in Fig. 2. The region shows a variable visual extinction, with a median value of 4.3 mag.

3.2. Young stellar population

Young Stellar Objects (YSOs) show an excess emission at infrared (IR) wavelengths above the bare photosphere due to thermal emission from their circumstellar dust envelopes. The re-emission by the cold dust envelope is more efficient at mid-IR wavelengths. Hence, a mid-IR
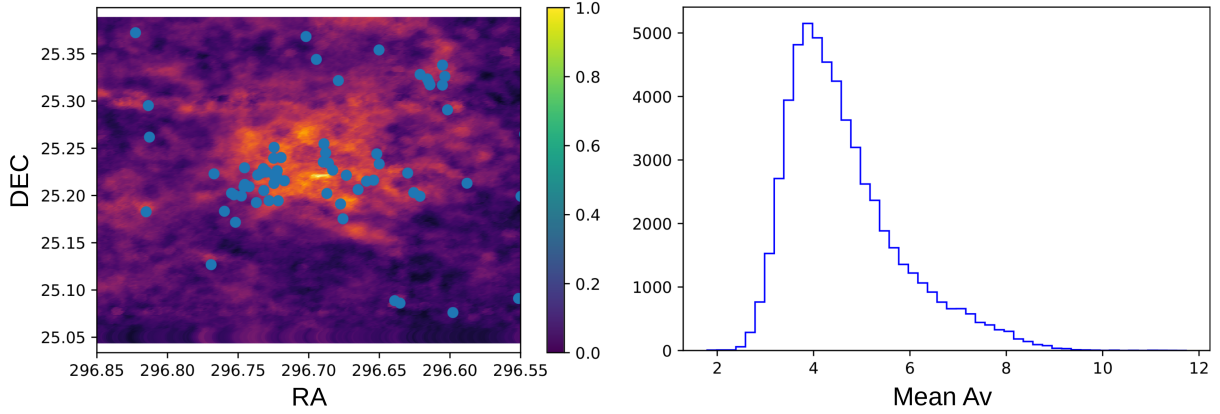
Figure 2: (*Left*) The visual extinction map of S88 over 20×20 arcminutes is displayed here, showing a variable extinction of the region. The blue dots indicate the positions of YSOs. (*Right*) Histogram plot of the region's extinction values (median: 4.3 mag).

survey of any star-forming region could be a powerful tool to distinguish the young stars with IR excesses from the foreground and background diskless population. According to evolutionary sequence, YSOs are categorized into Class 0, I, II, and III evolutionary stages (Lada and Wilking, 1984). The IR excesses of YSOs are high in Class 0 and I compared to Class II, while Class III stars are mostly diskless.

For YSOs classification, we have used data from the four *Spitzer*–IRAC bands ([3.6], [4.5], [5.8] and [8.0]) of S88 over the 20×20 arcminute region. After contamination removal, we classified the YSOs into Class I and II following Gutermuth et al. (2009), based upon the mid-IR colour criteria of the four IRAC bands. We found that six sources had mid-IR colours consistent with Class I, while 43 sources had mid-IR colours consistent with Class II. In the left-hand panel of Fig. 3, the colour-colour diagram of [3.6]–[4.5] vs. [5.8]–[8.0] is shown; Class I sources are displayed in red and Class II sources in blue.

Additional YSOs are detected from the dereddened $[[3.6] - [4.5]]_0$ vs. $[[K] - [3.6]]_0$ colour-colour diagram in the phase 2 classification scheme of Gutermuth et al. (2009) as a few YSOs are faint and undetected in the longer wavelength [5.8] and [8.0] IRAC bands. The dereddened $[[3.6] - [4.5]_0$ and $[[K] - [3.6]]_0$ colours are estimated from the extinction of the nearest grid point for that source. After removing YSOs selected from the four IRAC bands, 25 sources were found to have colours consistent with Class I. The right-hand panel of Fig. 3 shows the colour-colour diagram of $[[3.6] - [4.5]]_0$ versus $[[K] - [3.6]]_0$, with Class II sources displayed in blue. No Class I source was identified in this colour scheme.

Many young low-mass stars show an H_α emission from either chromospheric activity or circumstellar accretion. The IPHAS survey provides photometry of fainter emission line objects up to r and $i \leq 20.5$, and $H_\alpha \leq 19.5$ mag, with a photometric uncertainty of 0.1 mag (Barentsen et al., 2014). According to the $(r - i)$ versus $(r - H_\alpha)$ colour-colour criterion of Barentsen et al. (2014), 41 YSOs are identified as emission line stars (magenta squares); they are most probably Class II or Class III sources. Among these 41 H_α emitting YSOs, four are also characterized
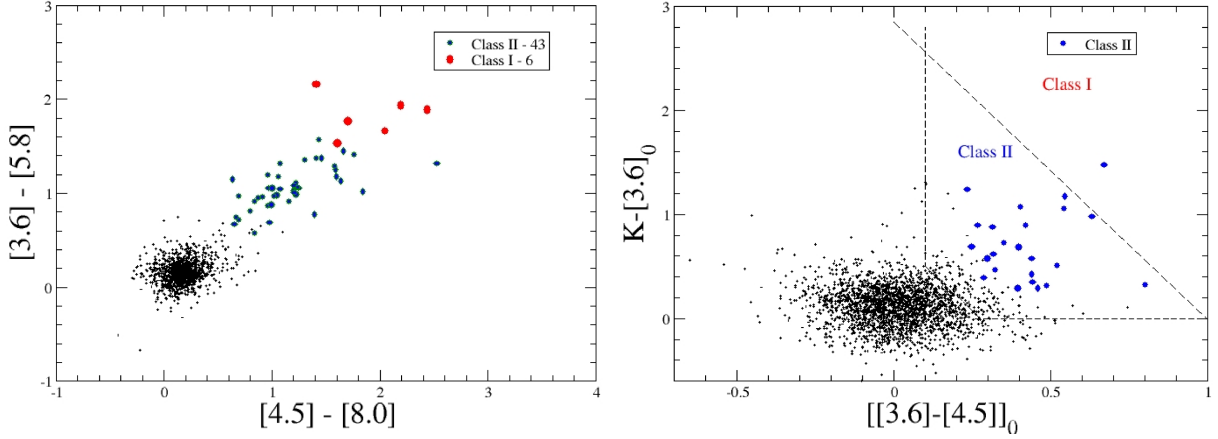
Figure 3: (*Left*) *Spitzer*–IRAC colour-colour diagram. This diagram shows the distribution of diskless and field stars (black dots), and Class II (blue circles) and Class I sources (red circles). (*Right*) The dereddened colour-colour diagram of $[[3.6] - -[4.5]]_0$ vs. $[[K] - -[3.6]]_0$ shows the background and foreground (black dots) as well as the Class II (blue circle) populations. The source classification scheme is adapted from Gutermuth et al. (2009).

from IR excesses using IRAC bands. In Fig. 4, 41 sources show $(r - H_\alpha)$ colours that are reflecting strong H_α line emitters. By contrast, the field star distribution shows two well-defined loci of stellar populations, one for the unreddened main sequence and the other for the giant stars (grey dots). Similar methods are studied previously in several star-forming regions (Dutta et al., 2015, 2018; Panja et al., 2020, 2021, 2022).

4. Summary and Conclusion

In this work, the census of YSOs in the young star-forming H II region, S88, are reported using infrared colour excesses from mid-IR *Spitzer*–IRAC and near-IR 2MASS data, and H_α emitters from the IPAHS photometric data. The H_α emitters are identified with IPHAS narrow-band H_α, as well as *r*- and *i*-band data. The visual extinction map of the region is generated using deep UKIDSS *H*- and *K*-band data.

- The visual extinction map covering 20×20 arcminutes around S88 is generated using deep UKIDSS *H* and *K*-band data. We find a sizeable variable extinction over the region of up to $A_V \simeq 11.7$ mag, with a median value of $A_V \simeq 4.3$ mag. The high extinction regions trace the dense filamentary structure, which was found earlier in the far-infrared and sub-mm data.

- Using the four *Spitzer* IRAC mid-IR bands and 2MASS K_s data, analysis of colour-colour diagrams are performed, and we have identified six Class I and 68 Class II YSOs.

- From IPHAS photometry data, 41 YSOs are identified as emission line stars. They are
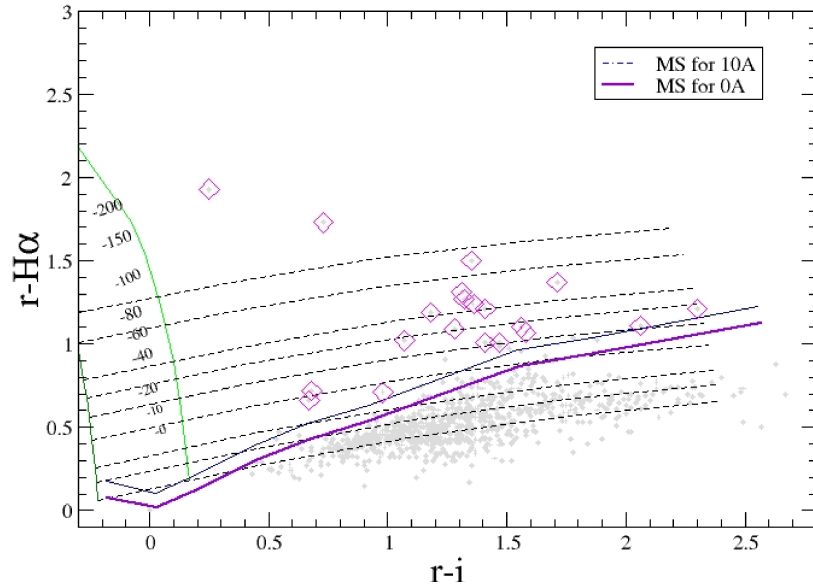
Figure 4: The magenta squares are YSOs with a spectroscopic H_α equivalent width (EW) stronger than $-10\,\text{Å}$. The solid line shows the simulated main-sequence (MS) curve at the mean reddening of the cluster; dashed lines show the positions of stars at increasing $H\alpha$ emission levels, as predicted by the simulated tracks; grey dots show field stars in the region.

probably Class II or Class III YSOs. Among these 41 H_α emitting YSOs, four are also characterized from IR excesses using IRAC bands.

Acknowledgments

Further Information

Authors' ORCID identifiers

0009-0008-2349-7677 (Soumita CHAKRABORTY)
0000-0003-1457-0541 (Soumen MONDAL)
0000-0002-4719-3706 (Alik PANJA)
0000-0001-7175-684X (Siddhartha BISWAS)

0000-0002-6990-5372 (Dorothy MUSEO MWANZIA)

0009-0007-1545-854X (Santosh JOSHI)

Author contributions

SC and SM carried out the extinction map and YSOs classification. The text was written by SC and SM. All authors contributed to the discussion and interpretation of the results and commented on the written draft of the paper.

Conflicts of interest

The authors declare no conflict of interest.

References

André, P., Di Francesco, J., Ward-Thompson, D., Inutsuka, S. I., Pudritz, R. E. and Pineda, J. E. (2014) From filamentary networks to dense cores in molecular clouds: Toward a new paradigm for star formation. In Protostars and Planets VI, edited by Beuther, H., Klessen, R. S., Dullemond, C. P. and Henning, T., pp. 27–51. https://doi.org/10.2458/azu_uapress_ 9780816531240-ch002.

Barentsen, G., Farnhill, H. J., Drew, J. E., González-Solares, E. A., Greimel, R., Irwin, M. J., Miszalski, B., Ruhland, C., Groot, P., Mampaso, A., Sale, S. E., Henden, A. A., Aungwerojwit, A., Barlow, M. J., Carter, P. J., Corradi, R. L. M., Drake, J. J., Eislöffel, J., Fabregat, J., Gänsicke, B. T., Gentile Fusillo, N. P., Greiss, S., Hales, A. S., Hodgkin, S., Huckvale, L., Irwin, J., King, R., Knigge, C., Kupfer, T., Lagadec, E., Lennon, D. J., Lewis, J. R., Mohr-Smith, M., Morris, R. A. H., Naylor, T., Parker, Q. A., Phillipps, S., Pyrzas, S., Raddi, R., Roelofs, G. H. A., Rodríguez-Gil, P., Sabin, L. and Scaring, S. and Steeghs, D. and Suso, J. and Tata, R. and Unruh, Y. C. and van Roestel, J. and Viironen, K. and Vink, J. S. and Walton, N. A. and Wright, N. J. and Zijlstra, A. A. (2014) The second data release of the INT Photometric Hα survey of the Northern Galactic Plane (IPHAS DR2). MNRAS, 444(4), 3230–3257. https://doi.org/10.1093/mnras/stu1651.

Benjamin, R. A., Churchwell, E., Babler, B. L., Bania, T. M., Clemens, D. P., Cohen, M., Dickey, J. M., Indebetouw, R., Jackson, J. M., Kobulnicky, H. A., Lazarian, A., Marston, A. P., Mathis, J. S., Meade, M. R., Seager, S., Stolovy, S. R., Watson, C., Whitney, B. A., Wolff, M. J. and Wolfire, M. G. (2003) GLIMPSE. I. An *SIRTF* Legacy Project to map the inner Galaxy. PASP, 115(810), 953–964. https://doi.org/10.1086/376696.

Billot, N., Noriega-Crespo, A., Carey, S., Guieu, S., Shenoy, S., Paladini, R. and Latter, W. (2010) Young stellar objects and triggered star formation in the Vulpecula OB association. ApJ, 712(2), 797–812. https://doi.org/10.1088/0004-637X/712/2/797.

Cappa, C., Pineault, S., Arnal, E. M. and Cichowolski, S. (2002) An H I interstellar bubble linked to the O-type stars BD +24°3866 and BD +25°3952. A&A, 395, 955–967. https://doi.org/10.1051/0004-6361:20021304.

Deharveng, L., Zavagno, A. and Caplan, J. (2005) Triggered massive-star formation on the borders of Galactic H II regions. I. A search for "collect and collapse" candidates. A&A, 433(2), 565–577. https://doi.org/10.1051/0004-6361:20041946.

Drew, J. E., Greimel, R., Irwin, M. J., Aungwerojwit, A., Barlow, M. J., Corradi, R. L. M., Drake, J. J., Gänsicke, B. T., Groot, P., Hales, A., Hopewell, E. C., Irwin, J., Knigge, C., Leisy, P., Lennon, D. J., Mampaso, A., Masheder, M. R. W., Matsuura, M., Morales-Rueda, L., Morris, R. A. H., Parker, Q. A., Phillipps, S., Rodriguez-Gil, P., Roelofs, G., Skillen, I., Sokoloski, J. L., Steeghs, D., Unruh, Y. C., Viironen, K., Vink, J. S., Walton, N. A., Witham, A., Wright, N., Zijlstra, A. A. and Zurita, A. (2005) The INT photometric Hα Survey of the Northern Galactic Plane (IPHAS). MNRAS, 362(3), 753–776. https://doi.org/10.1111/j.1365-2966.2005.09330.x.

Dutta, S., Mondal, S., Jose, J., Das, R. K., Samal, M. R. and Ghosh, S. (2015) The young cluster NGC 2282: a multiwavelength perspective. MNRAS, 454(4), 3597–3612. https://doi.org/10.1093/mnras/stv2190.

Dutta, S., Mondal, S., Samal, M. R. and Jose, J. (2018) The *Planck* Cold Clump G108.37-01.06: A site of complex interplay between H II regions, young clusters, and filaments. ApJ, 864(2), 154. https://doi.org/10.3847/1538-4357/aadb3e.

Fazio, G. G., Hora, J. L., Allen, L. E., Ashby, M. L. N., Barmby, P., Deutsch, L. K., Huang, J. S., Kleiner, S., Marengo, M., Megeath, S. T., Melnick, G. J., Pahre, M. A., Patten, B. M., Polizotti, J., Smith, H. A., Taylor, R. S., Wang, Z., Willner, S. P., Hoffmann, W. F., Pipher, J. L., Forrest, W. J., McMurty, C. W., McCreight, C. R., McKelvey, M. E., McMurray, R. E., Koch, D. G., Moseley, S. H., Arendt, R. G., Mentzell, J. E., Marx, C. T., Losch, P., Mayman, P., Eichhorn, W., Krebs, D., Jhabvala, M., Gezari, D. Y., Fixsen, D. J., Flores, J., Shakoorzadeh, K., Jungo, R., Hakun, C., Workman, L., Karpati, G., Kichak, R., Whitley, R., Mann, S., Tollestrup, E. V., Eisenhardt, P., Stern, D., Gorjian, V., Bhattacharya, B., Carey, S., Nelson, B. O., Glaccum, W. J., Lacy, M., Lowrance, P. J., Laine, S., Reach, W. T., Stauffer, J. A., Surace, J. A., Wilson, G., Wright, E. L., Hoffman, A., Domingo, G. and Cohen, M. (2004) The Infrared Array Camera (IRAC) for the *Spitzer Space Telescope*. ApJS, 154(1), 10–17. https://doi.org/10.1086/422843.

Flaherty, K. M., Pipher, J. L., Megeath, S. T., Winston, E. M., Gutermuth, R. A., Muzerolle, J., Allen, L. E. and Fazio, G. G. (2007a) Infrared extinction toward nearby star-forming regions. ApJ, 663(2), 1069–1082. https://doi.org/10.1086/518411.

Flaherty, K. M., Pipher, J. L., Megeath, S. T., Winston, E. M., Gutermuth, R. A., Muzerolle, J., Allen, L. E. and Fazio, G. G. (2007b) Infrared extinction toward nearby star-forming regions. ApJ, 663(2), 1069–1082. https://doi.org/10.1086/518411.

Fukuda, N. and Hanawa, T. (2000) Sequential star formation triggered by expansion of an H II region. ApJ, 533(2), 911–923. https://doi.org/10.1086/308701.

Gutermuth, R. A., Megeath, S. T., Myers, P. C., Allen, L. E., Pipher, J. L. and Fazio, G. G. (2009) A *Spitzer* survey of young stellar clusters within one kiloparsec of the Sun: Cluster core extraction and basic structural analysis. ApJS, 184(1), 18–83. https://doi.org/10.1088/0067-0049/184/1/18.

Gutermuth, R. A., Megeath, S. T., Pipher, J. L., Williams, J. P., Allen, L. E., Myers, P. C. and Raines, S. N. (2005) The initial configuration of young stellar clusters: A *K*-band number counts analysis of the surface density of stars. ApJ, 632(1), 397–420. https://doi.org/10.1086/432460.

Kennicutt, R. C. and Evans, N. J. (2012) Star formation in the Milky Way and nearby galaxies. ARA&A, 50, 531–608. https://doi.org/10.1146/annurev-astro-081811-125610.

Kohno, M., Omodaka, T., Handa, T., Chibueze, J. O., Nagayama, T., Burns, R. A., Murase, T., Matsusaka, R., Nakano, M., Sunada, K., Yamada, R. I. and Bieging, J. H. (2022) Ammonia mapping observations toward the Galactic massive star-forming region Sh 2-255 and Sh 2-257. PASJ, 74(3), 545–556. https://doi.org/10.1093/pasj/psac014.

Lada, C. J. and Wilking, B. A. (1984) The nature of the embedded population in the rho Ophiuchi dark cloud: mid-infrared observations. ApJ, 287, 610–621. https://doi.org/10.1086/162719.

Lawrence, A., Warren, S. J., Almaini, O., Edge, A. C., Hambly, N. C., Jameson, R. F., Lucas, P., Casali, M., Adamson, A., Dye, S., Emerson, J. P., Foucaud, S., Hewett, P., Hirst, P., Hodgkin, S. T., Irwin, M. J., Lodieu, N., McMahon, R. G., Simpson, C., Smail, I., Mortlock, D. and Folger, M. (2007) The UKIRT Infrared Deep Sky Survey (UKIDSS). MNRAS, 379(4), 1599–1617. https://doi.org/10.1111/j.1365-2966.2007.12040.x.

McKee, C. F. and Ostriker, E. C. (2007) Theory of star formation. ARA&A, 45, 565–687. https://doi.org/10.1146/annurev.astro.45.051806.110602.

Morgan, W. W., Whitford, A. E. and Code, A. D. (1953) Studies in galactic structure. I. A preliminary determination of the space distribution of the blue giants. ApJ, 118, 318. https://doi.org/10.1086/145754.

Panja, A., Chen, W. P., Dutta, S., Sun, Y., Gao, Y. and Mondal, S. (2021) Sustaining star formation in the Galactic star cluster M 36? ApJ, 910(1), 80. https://doi.org/10.3847/1538-4357/abded4.

Panja, A., Mondal, S., Dutta, S., Joshi, S., Lata, S. and Das, R. (2020) Census of the young stellar population in the Galactic H II region Sh2-242. AJ, 159(4), 153. https://doi.org/10.3847/1538-3881/ab737a.

Panja, A., Sun, Y., Chen, W. P. and Mondal, S. (2022) Star and cluster formation in the Sh2-112 filamentary cloud complex. ApJ, 939(1), 46. https://doi.org/10.3847/1538-4357/ac940f.

Rieke, G. H. and Lebofsky, M. J. (1985) The interstellar extinction law from 1 to 13 microns. ApJ, 288, 618–621. https://doi.org/10.1086/162827.

Sharpless, S. (1959) A catalogue of H II regions. ApJS, 4, 257. https://doi.org/10.1086/190049.

Skrutskie, M. F., Cutri, R. M., Stiening, R., Weinberg, M. D., Schneider, S., Carpenter, J. M., Beichman, C., Capps, R., Chester, T., Elias, J., Huchra, J., Liebert, J., Lonsdale, C., Monet, D. G., Price, S., Seitzer, P., Jarrett, T., Kirkpatrick, J. D., Gizis, J. E., Howard, E., Evans, T., Fowler, J., Fullmer, L., Hurt, R., Light, R., Kopan, E. L., Marsh, K. A., McCallon, H. L., Tam, R., Van Dyk, S. and Wheelock, S. (2006) The Two Micron All Sky Survey (2MASS). AJ, 131(2), 1163–1183. https://doi.org/10.1086/498708.

Walch, S., Whitworth, A. P., Bisbas, T. G., Wünsch, R. and Hubber, D. A. (2013) Clumps and triggered star formation in ionized molecular clouds. MNRAS, 435(2), 917–927. https://doi.org/10.1093/mnras/stt1115.